

Supplemental Material S1. Laryngeal displacement device (LDD): Video laryngoscopy.

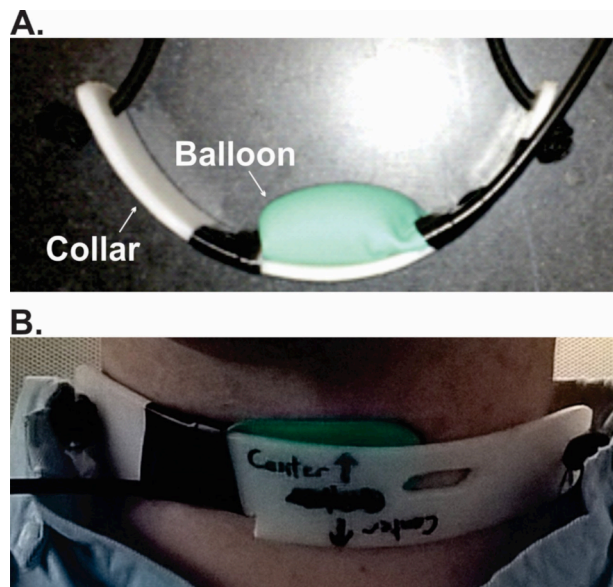


Figure S1: The collar and balloon of the LDD. Panel A depicts the balloon fully inflated. Panel B depicts the balloon fully deflated and fitted to an experimenter's neck.

A subset of five participants took part in a laryngoscopic investigation of the laryngeal perturbation task. The experimental setup was the same as Experiment 1, with the addition of a flexible endoscope (Digital Stroboscopy System; Kay Elemetrics), a Kay-Pentax lapel microphone, and a halogen light source. Participants were given five pumps of Afrin nasal decongestion spray to clear the nasal passage, and lubricant was applied to the endoscope to aid insertion. The endoscope was inserted through the right nostril, past the velopharyngeal port, and placed just above the back of the tongue in order to capture the motions of the laryngeal anatomy during the task. The endoscope was held at a height just behind the back of the tongue to view the full anatomy of the epiglottis, arytenoids, and pyriform sinus. Digital video data were collected at 30 fps with 720×540 pixel-sized frames and were recorded in tandem with the audio data. Participants completed 10 trials of the vocalization task (as in Experiment 1) and had the laryngeal perturbation applied on all 10 trials.

Each trial of the laryngoscopy session had a video of length of 120 frames (4 s at 30 fps). Ten trials were collected for each participant. From this set, 5 videos were chosen from each participant based on the following criteria: (i) minimal frame-to-frame movement of the visual scene due to scope movement; (ii) significant coverage of laryngeal structures in every frame; (iii) minimal distance from the larynx (i.e., maximum size of the laryngeal structures in the images), and (iv) noticeable movement of the laryngeal structures relative to the surrounding tissue over the course of the trial. Inspection of the resulting videos indicated that the primary perturbation-induced effect visible from the scope was an expansion of the size of arytenoids in the image, consistent with upward movement (toward the scope). We speculate that this upward movement (seen in most participants) at the top of the larynx is the result of a rostrally oriented rotation of the larynx induced by posterior movement at the laryngeal prominence, but the limited view from the scope is insufficient to verify this speculation. Nonetheless, the visible expansion of the laryngeal structures during perturbation provides a measure of the gross effect of the perturbation that is sufficient for eliminating the possibility that compensatory pitch

adjustments were simply due to the larynx returning to its starting position shortly after perturbation onset.

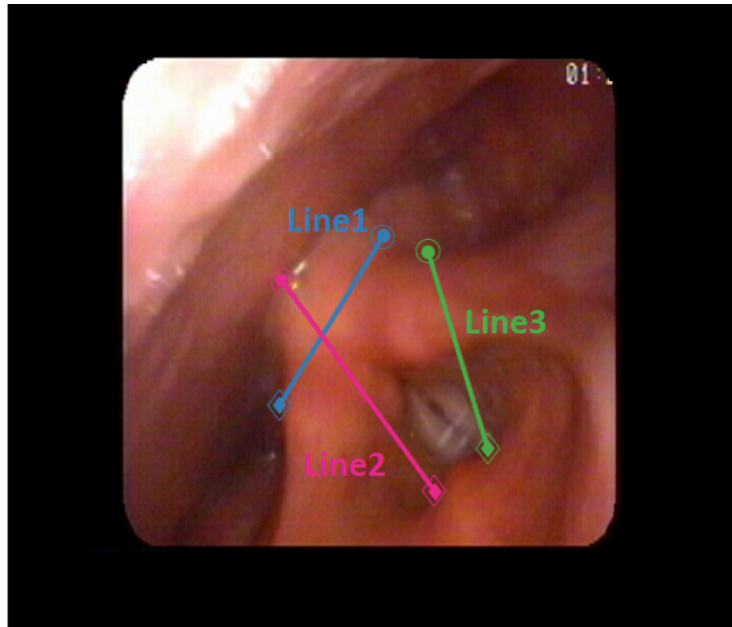


Figure S2: Example video frame from the fiduciary point coding procedure. The three-line segments are defined by three sets of points that are marked in subsequent frames. The change in length of the line segments is tracked across frames within a trial.

We developed a procedure aimed at quantifying the enlargement of the laryngeal structures in the images that occurred due to upward movement. To begin this procedure, a single video coder first watched a given video (trial) in real time to identify candidate fiduciary points on the visible laryngeal structures that met two criteria: (i) the fiduciary point was clearly identifiable in all frames of the video, and (ii) it displayed variation in position over the course of the trial. The coder was asked to choose three pairs of such points on the first frame of the video; each pair of points defining a line segment; Line1, Line2, and Line3 (see example frame in Figure S2). The coder then manually scrolled through the video, frame by frame, and marked the new position of the fiduciary points in the subsequent frames. As the position of the fiduciary points changed between frames, the length of the line segments (in pixels) also changed. Ultimately, a fully coded trial described the time series change in length of each line segment, which captured a general measure of the laryngeal movement present in the trial. Due to substantial cross-participant and cross-trial variability in which anatomical structures were visible, it was not possible to use fiduciary points corresponding to the same anatomical structures in all videos. The choice of three pairs of fiduciary points per trial, rather than a single pair, was made to decrease sensitivity to small errors in identifying the same point in every frame of the video and to increase overall coverage of the laryngeal structures when calculating the movement index. The coder was blind to onset/offset time of the perturbation during the manual coding process, but was given the perturbation onset/offset time information when viewing the real-time video during fiduciary point selection.

The time series for each line segment were time aligned with respect to the onset of perturbation and cropped to a window extending 500 ms before perturbation to 1000 ms after. Each time series was then smoothed with a 0.1 s sliding window, and the baseline length of the line segment was estimated as the mean length in the 15 frames (500 ms) preceding the onset of

laryngeal perturbation. Finally, each line segment time series was zero-meaned by subtracting its baseline length from the measured length at each frame in the trial. This process was repeated for all five trials per participant, and the time-series length measurements of all line segments were averaged across trials, and then averaged across line segments, and finally averaged across all participants. The culmination of these averages produced a single measure of gross laryngeal movement (*movement index*) as a function of time relative to perturbation onset. A subset of 3 trials from three different participants were re-coded by the same coder (12% of the originally coded trials; starting from the same initial fiducial points in the initial frame) to obtain a measure of intra-rater reliability. Reliability was assessed using a Pearson's correlation between the value of the Euclidian distance measured in the first and second coding sessions. The intra-coder reliability was found to be strongly correlated ($r = 0.99$, $p < .001$), with a mean difference of 2.38 pixels ($SD = 5.66$ pixels) between coding sessions.

The mean movement index is plotted in Figure S3 (aligned to perturbation onset). Despite the relatively coarse nature of the movement measures, the movement index (in blue) clearly indicates a distinct pattern of movement compared to the corresponding f_0 traces (magenta): whereas the mean f_0 trace reverses direction back toward baseline after initial displacement due to the perturbation, the mean length of the fiducial line segments increases monotonically after perturbation onset.

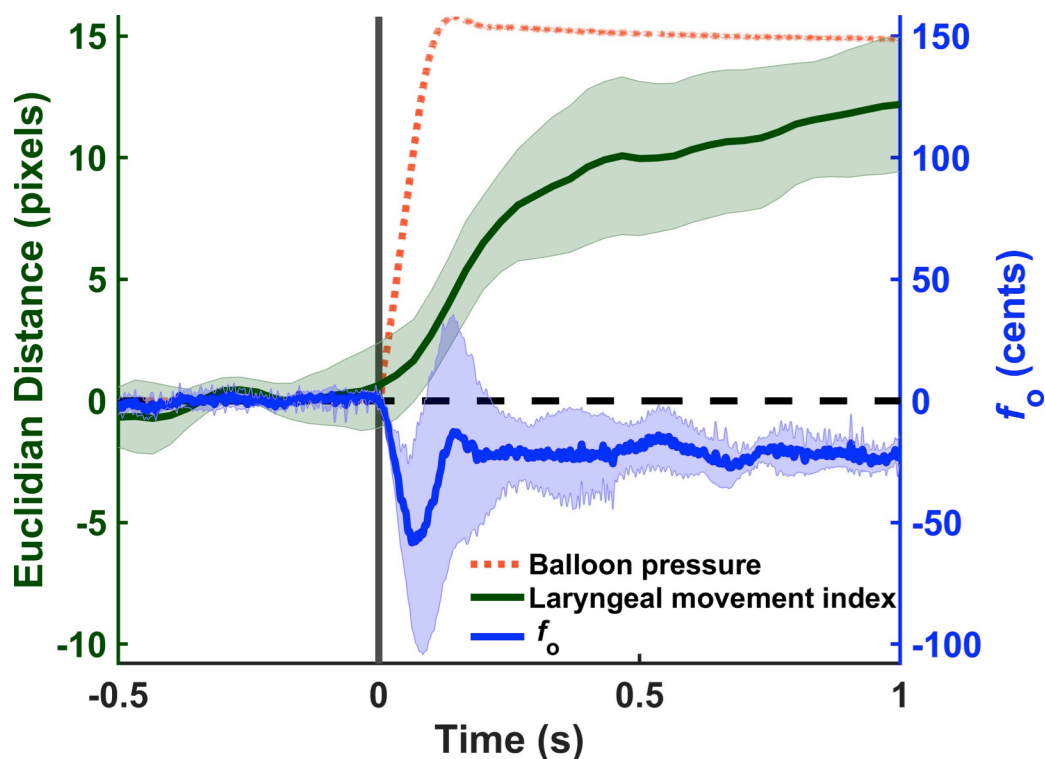


Figure S3: Mean laryngeal movement index (green line) aligned to the onset of the LDD inflation (vertical line) contrasted with the mean change in f_0 (blue line). The perturbation remains on through the entire period of 1 s following perturbation onset. Shading indicates 95% confidence interval. The orange trace represents the mean pressure inside the balloon during all perturbed trials (units not shown, but range from 0 to 3.8 psi).